P 2.4 **THE HISTORIC CHRISTMAS 2004 SOUTH TEXAS SNOW EVENT: DIAGNOSIS OF THE HEAVY SNOW BAND**

(Online version updated/corrected 07/31/2007)

Ronald F. Morales Jr.
National Weather Service, Corpus Christi, TX

1. INTRODUCTION

On 24 and 25 December 2004, much of south Texas received a record snowfall. Measurable snow was reported from the Galveston/Houston region, southward to Corpus Christi, Brownsville and into Northeastern Mexico (Fig. 1). Embedded within the larger snow field was a narrow, heavier snow band. This band had maximum snow depths of 33 cm (13 inches), a half width (distance between maximum snowfall and half that amount) of approximately 48-64 km (30-40 miles), and a total length of more than 320 km (200 miles). Although Figure 1 reveals only one heavy snow band, a composite of the radar data from Weather Surveillance Radar-1988 (WSR-88D) sites across south Texas indicated that there were at least two distinct bands that formed during this event. The entire snow event occurred between the hours of 0000 and 1200 UTC 25 December, with the heaviest snow falling between 0200 to 0800 UTC. Maximum snowfall rates of 5 to 10 cm h^{-1} (2 to 4 inches h^{-1}) were observed within the heavy snow band region.

To put this Christmas 2004 snow event into historical perspective, the last time many locations across south Texas had recorded snowfall amounts greater than or equal to those received in this storm was back in the late 1800s. For example, Corpus Christi (not in the heavy snow band) and Victoria had not received such a snowfall since February 1895. It was also the first ever recorded Christmas Day snowfall for Victoria (Wilk et al, 2007). Many locations from the Houston/Galveston area, southward to the lower Rio Grande Plains and northeast Mexico, recorded their first white Christmas since local records began (NCDC Storm Data, Dec. 2004). The

* *Corresponding author address*: Ronald F. Morales Jr., National Weather Service, 300 Pinson Dr., Corpus Christi, TX 78406; e-mail: ron.morales@noaa.gov

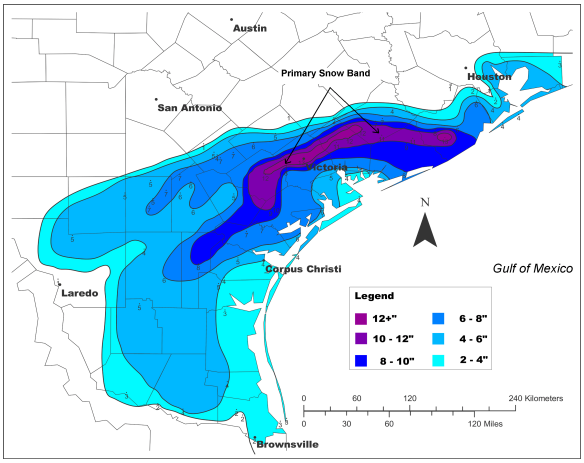

Figure 1. Snowfall analysis (inches) depicting the heavy snow band.

February 1895 snow event also produced a narrow band of snow across south and southeast Texas, but the snow totals were nearly double (10-20 inches) those of the current case (Griffiths and Ainsworth, 1981). Snowfall amounts were likely higher with the 1895 storm simply because it lasted much longer (three days) than the 2004 event, which persisted for only 8 to 12 hours.

The primary motivation for this study was to diagnose the potential cause(s) for the narrow heavy snow band, which was not predicted by any of the operational numerical models, even up to the time of the event. Since such a winter event requires the presence of a deep, sufficiently cold environment to produce frozen precipitation, a brief investigation into the origin and maintenance of the deep cold air mass was also included. Overall, it is expected that this study will reveal that, despite the rare snow totals and deep cold air mass across low latitudes, the associated dynamics were not necessarily unique when compared to other more northern, narrow heavy snow band events.

2. DATA AND METHODOLOGY

All of the data used for this study were taken from local archives produced from the National Weather Service's Advanced Weather Interactive Processing System (AWIPS) at the National Weather Service Forecast Office (NWSFO), Corpus Christi. Since this study was intended to benefit operational forecasters, it seemed appropriate to utilize the data that was operationally available to the affected south Texas NWSFOs. The 80 km North American Mesoscale Eta (NAM-Eta) model, initialized at 0000 UTC 25 December, was used to diagnose the synoptic environment.

To diagnose the possible cause(s) for the heavy band of snow, cross sections of Petterssen frontogenesis, saturated equivalent potential geostrophic vorticity (EPV*), saturated equivalent potential temperature (θ_{es}), omega, and relative humidity were constructed perpendicular to the heavy snow band. This method was similar to that used by Nicosia and Grumm (1999), Novak et al. (2002), Schumacher (2003), and Jurewicz and Evans (2004). The cross sections were generated using the Local Analysis and Prediction System (LAPS) on AWIPS (Albers et al 1996). The LAPS output was desirable, since it was available hourly over a regional domain with a horizontal grid resolution of 10 km. For this case study, the LAPS analyses were centered on the Corpus Christi Forecast Office's area of responsibility across south Texas (Fig. 2), which coincided with the region of the primary heavy snow band.

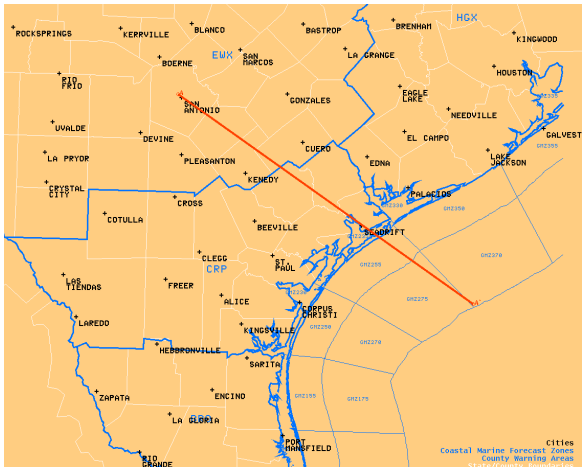

Figure 2. Boundaries of NWS County Warning Areas (CWAs) in blue. Red line denotes cross section location used to diagnose the snow band.

In order to track the snow band evolution, reflectivity data were utilized mainly from three National Weather Service Doppler radars (88Ds) across the area, including: Corpus Christi (KCRP), Brownsville (KBRO), and Austin/San Antonio (KEWX) (see Fig. 6). The AWIPS dataset used for this case also contained composited (referred to as "mosaic" in the NWS) reflectivity data of the radar sites listed above. These composited reflectivity products made it possible to view a much larger geographic region than could be viewed by just one radar at a given time. The storm total precipitation (STP) products from the three WSR-88Ds were also very helpful in locating the heavy snow bands.

The snowfall data were compiled and hand analyzed from cooperative observers, Automated Surface Observing Systems (ASOS), and from reports by public and law enforcement officials. Most of the snowfall data appeared to be accurate. However, when discrepancies existed, particularly within the suspected regions of heavier snowfall, the data were either discarded or estimated using the ratio of liquid water to snowfall reported by the Victoria cooperative observer. The Victoria observer was trained by National Weather Service personnel to properly measure snowfall and the liquid equivalent.

3. SYNOPTIC AND MESOSCALE OVERVIEW

a. LARGE SCALE PATTERN

The discussion of the significant synoptic features associated with this storm will cover the period between 0000 and 1200 UTC 25 December, which coincided with main time frame of the snow event. The heaviest snowfall occurred generally between 0200 and 0800 UTC 25 December. Additional details on the synoptic scale features out to 48 hours prior to the beginning of the banded snow event can be found at Wilk et al (2007).

At 0000 UTC 25 December, the upper level pattern exhibited a deep layer ridge axis over the Pacific Northwest of the United States, with a split flow pattern downstream over the central U.S., southward to Mexico (Fig. 3, top panels). The upper trough within the southern stream branch of the flow was beginning to close off over northern Mexico, with a positively tilted northern stream trough axis extending from the Great Lakes region, southwest into the southern plains. Along

the eastern sides of the two upper troughs was an upper level jet centered around 250 hPa, which had two embedded jet maxima between the mid-Atlantic coast and northern Mexico (Fig. 3, top left). The strongest jet core was over the Tennessee River Valley and the mid Atlantic states, with maximum speeds of 93-103 m s^{-1} (180-200 kts). A secondary jet core of 72-77 m s^{-1} (140-150 kts) ran across northern Mexico and southern Texas. This configuration placed much of southern and eastern Texas (the region of the eventual heavy snow band) in the exit region of the southern-most upper jet streak, and the entrance region of the northern one.

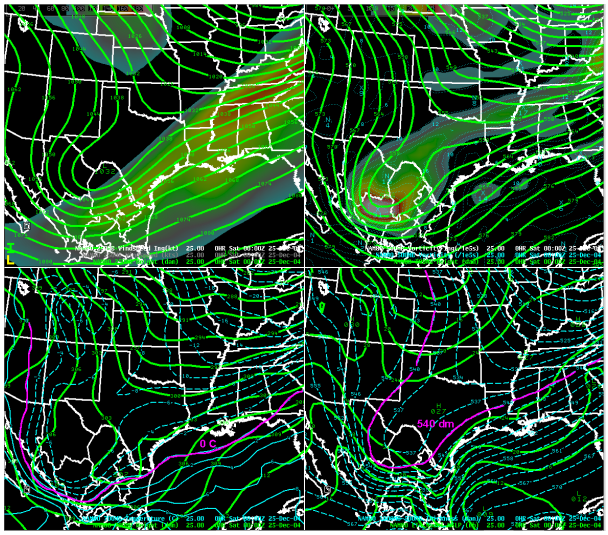

Figure 3. (Top left): 250 hPa height (dm) and wind speed (kts, ≥ 40 m s^{-1} shaded); (Top Right): 500 hPa height (dm) and absolute vorticity ($\geq 10\times10^{-5}$ s^{-1} shaded); (Bottom Left): 700 hPa height (dm) and temperature (˚C), pink contour denoting 0˚C isotherm; (Bottom Right): Sea level pressure and 1000-500 hPa thickness (dm), pink line denoting the 540 dm thickness contour. Valid at 0000 UTC 25 December.

At the lower and middle levels of the atmosphere, the noteworthy features were the depth of freezing/sub-freezing air and the lack of any significantly strong surface cyclone or anti-cyclone (Fig. 3, bottom panels). The 700 hPa analyses showed that the 0˚C isotherm had pushed down to the border of Texas and Mexico (Fig. 3, bottom left). At the surface, where temperatures (not shown) were in the 0 to 3˚C range (lower to mid 30s˚F), there was a weak ridge of high pressure, with a long east-west axis from northern Mexico, northeast into the Ohio River Valley. This ridge axis was the remnant high pressure area left behind by the arctic air mass that initiated the deep cold push of air into south Texas early on 23 December (not shown). There was a weak surface cyclone (central pressure around 1009 hPa) over the southwest Gulf of Mexico, which was approximately 835 to 925 km (450 to 500 nautical miles) southeast of the eventual heavy snow band (Fig. 3, bottom right). Between the surface cyclone well offshore to the east, and a ridge of higher pressure over northern and central Texas, the entire south Texas region was under the influence of low level northwesterly flow.

By 1200 UTC 25 December (the end of the event), upper level analyses indicated a low center over south Texas, near Corpus Christi (Fig. 4, top panels). The split upper flow noted 12 hours earlier continued, with the strongest upper level jet at 250 hPa (82-85 m/s, 160-165 knots) now concentrated on the east side of the northern stream flow over the southeast U.S. and mid Atlantic regions. Deep cold air from the surface to aloft remained over all of south Texas, with 700 hPa temperatures ranging between -4 to -6˚C, and surface temperatures (not shown) a bit lower than the previous 12 hours, -1 to +1˚C (upper 20s to lower 30s ˚F). The weak surface low also continued to translate eastward, now approaching the central Gulf of Mexico, with a high pressure ridge axis stretching from New England, southwest to central Texas. A surface cyclonic circulation was not observed for the event over south Texas within the vicinity of the heavy snow band region.

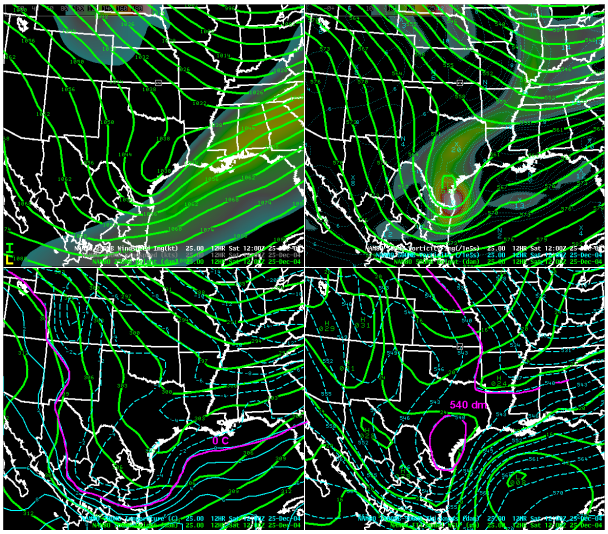

Figure 4. As in Fig. 3, except for 1200 UTC.

b. SATELLITE FEATURES

Beginning at 0000 UTC 25 December, the water vapor imagery indicated some upper level moisture near the upper low over northern Mexico and southern Texas (Fig. 5a). A dry slot was seen around the south and east side of the upper low, which included southern Texas. The brightest enhancement/best moisture was east of the land region of south Texas, over the western and northern Gulf of Mexico. The infrared (IR) imagery showed similar features (Fig. 5b). Of particular interest was the orientation of the cloud and moisture features in both the water vapor and IR data. For example, the clouds east of the upper low over south Texas were oriented east to west, while closer to the upper low, they were more northeast to southwest.

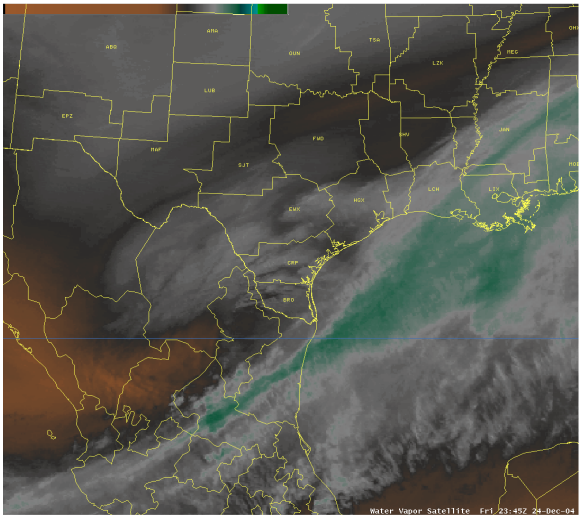

(a)

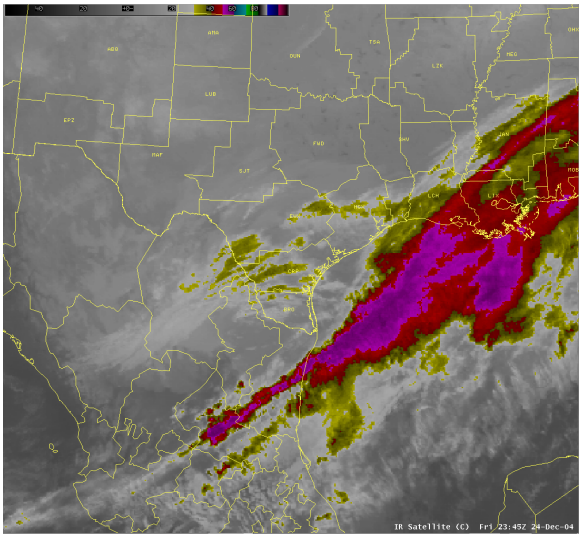

(b)

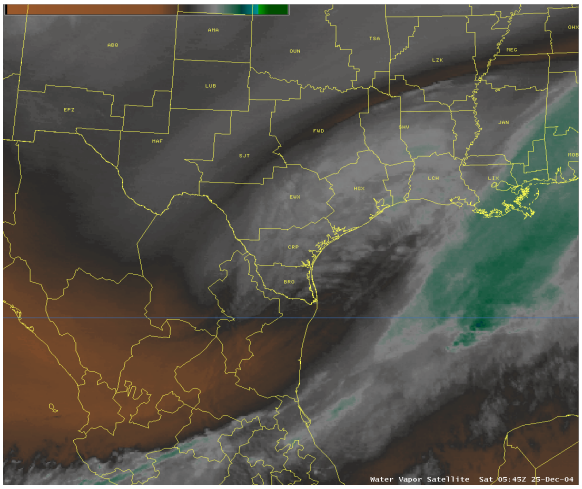

(c)

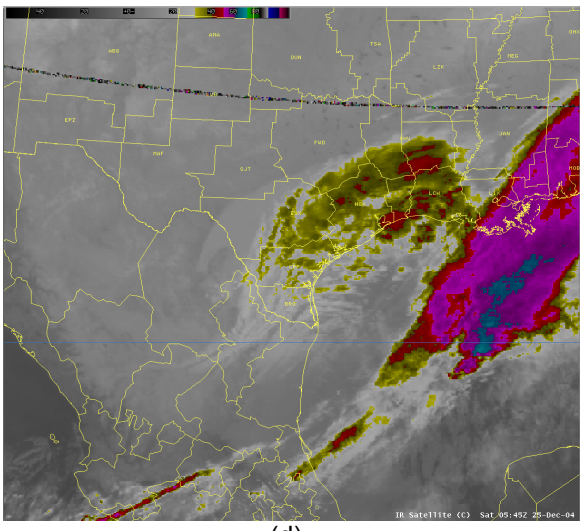

(d)

Figure 5. Water Vapor imagery (a, c) and Infrared (IR) imagery (b, d), valid at 0000 UTC (a, b), and 0600 UTC (c, d) 25 December. Drier regions are orange or black

As the upper low continued to move eastward toward south Texas, the cloud features became oriented more northeast to southwest by 0600 UTC (Figs. 5c, d). Cloud top temperatures, as depicted by the IR imagery, changed very little over south Texas during the period between 0000 and 0600 UTC (the peak period of heavy snow). The coldest cloud tops remained well offshore over the Gulf of Mexico. These colder tops were associated with the main upper jet core discussed above. Around 0600 UTC, the pattern in the satellite data appeared to indicate "cold air cyclogeneis" over south Texas, as the warm conveyor belt moisture over the western Gulf of Mexico moved west-northwest toward east Texas. This would suggest that lower level cyclogenesis may have been occurring over south and east Texas at this time, but none was observed. A detailed discussion concerning the potential implications of "cold air cyclogenesis" are beyond the scope of this paper. All of the features present at 0600 UTC seemed to remain intact and generally translate eastward away from the region by 1200 UTC (not shown).

c. RADAR TRENDS

The radar data around 0000 UTC 25 December indicated that the precipitation was dominated by convection over the eastern portions of south Texas (Fig. 6a). Convective bands were oriented east to west (black circle Fig. 6a), with embedded higher reflectivity values of 35-45 dBz, especially over the coastal counties of south Texas and the western Gulf of Mexico. The National Lightning Detection Network (NLDN) data even indicated a few cloud to ground (CG) strikes within the convective regions of higher reflectivity. Despite the very few CG strikes over the land areas throughout this event, reports from residents across the coastal region of south Texas confirmed the presence of periodic "rumbles" of thunder, especially early in the event between 0000 and 0200 UTC.

The transition to stratiform precipitation over the land areas of south Texas seemed to occur around 0200 UTC (Fig. 6b), with the convective regions now moving eastward into the western Gulf waters. Also by this time, at least two distinct bands of moderate to heavy snow were developing within the regions labeled as "developing primary" and "developing secondary" bands. The secondary band, located about 48 km (30 miles) northwest of the center of the primary band, was not clearly evident in the final snowfall analysis shown in figure 1 due to its shorter duration as compared to the primary band. This resulted in snowfall totals of approximately 40% lower in the secondary band.

Between 0400 and 0600 UTC, the secondary (northern) heavy snow band weakened and/or merged into the location of the primary band, which became the dominant band through the end of the event (Figs. 6c, d). The primary band weakened and began to move eastward offshore between 0800 and 1000 UTC (not shown). As the radar images indicated, the heaviest snow in the banded region(s) occurred between 0200 and 0800 UTC 25 December (six hours). This was a time scale very similar to those observed for many other heavy banded snow cases in the refereed literature.

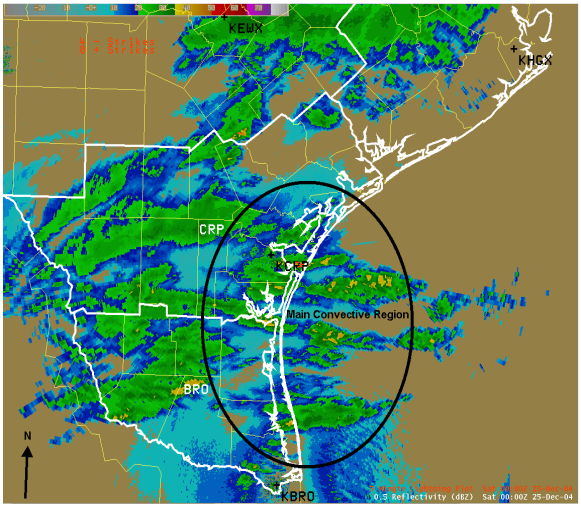

(a)

Figure 6. Radar reflectivity composite valid at 0000 UTC 25 December. Heavy snow bands depicted by black lines. County warning Areas of NWS office outlined in white lines (CRP = Corpus Christi, BRO = Brownsville). CG lightning data is in red. Black circle denotes main convective region at this time.

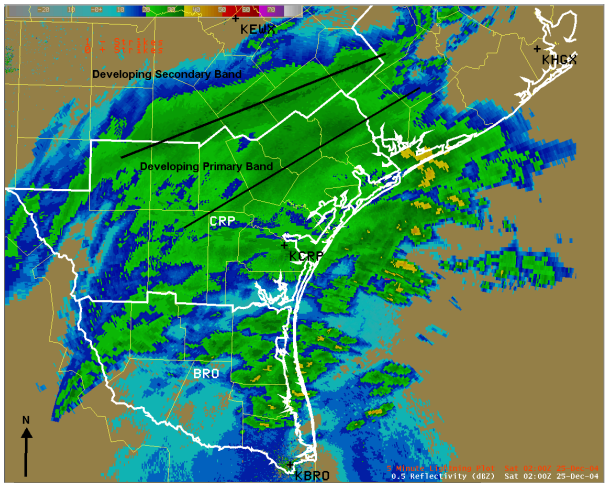

(b)

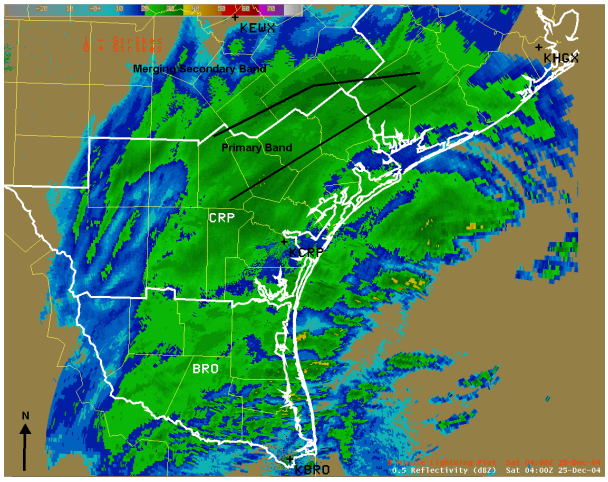

(c)

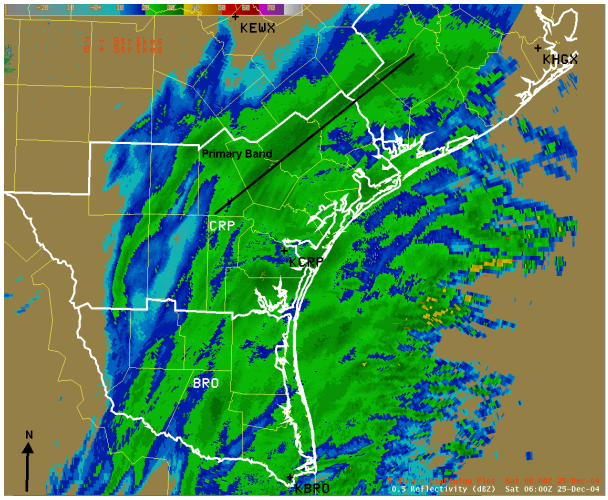

(d)

Figure 6 (Continued). Valid at (b) 0200, (c) 0400, and (d) 0600 UTC, 25 December.

d. THE PRESENCE AND MAINTENANCE OF DEEP COLD AIR

During the late afternoon hours of 24 December, just prior to the onset of the heavy snow, cloudy and breezy conditions prevailed, with surface temperatures holding around 1-2˚C across all of south Texas. Northwesterly low level flow maintained a continuous supply of cold, dry air across the area. Figure 7 shows an example of the surface conditions at 2100 UTC 24 December, which was a few hours prior to the onset of the event. The magnitude of the low level dry air was evident from observations of surface dew point temperatures, which ranged from -12˚C (10˚F) over central Texas, to -1˚C (30˚F) near the Texas/Mexico line. The 1200 UTC 24 December Corpus Christi (CRP) sounding (the sounding closest to the eventual heavy snow band region) revealed that the low level drier air was confined to below 950 hPa, with saturated, sub-freezing conditions up to 650 hPa (Fig. 8). Even though the 1200 UTC sounding indicated deep sub-freezing temperatures, the flow veered quickly from northerly at low levels, to southwesterly around 850 hPa and above, which indicated the presence of warm advection above 850 hPa. However, despite strong southwest flow of 15-20 m s^{-1} above 850 hPa at this time, there was only weak warm advection of 1-3˚C 12 h^{-1} in the layer between 850 and 500 hPa (Fig. 9). At lower levels, a mix of light (non-accumulating) precipitation fell into a relatively dry boundary layer late in the afternoon of the 24th, allowing evaporative cooling to lower temperatures to around 0˚C near the surface (not shown).

By 0000 UTC 25 December, the precipitation increased in coverage and intensity. The CRP sounding at this time continued to show dry low level conditions, and a deep freezing/sub-freezing saturated layer up to around 600 hPa, which was 100 hPa higher than the previous 12 hours (Fig. 10). There was a slight warming of 1-2˚C between 700 and 800 hPa, which was likely the result of weak warm advection during the day on the 24th discussed earlier. However, this elevated warm layer was relatively shallow (less than 700 meters), and the northerly flow had now deepened another 100 hPa to around 800 hPa (compare Figs. 8 and 10).

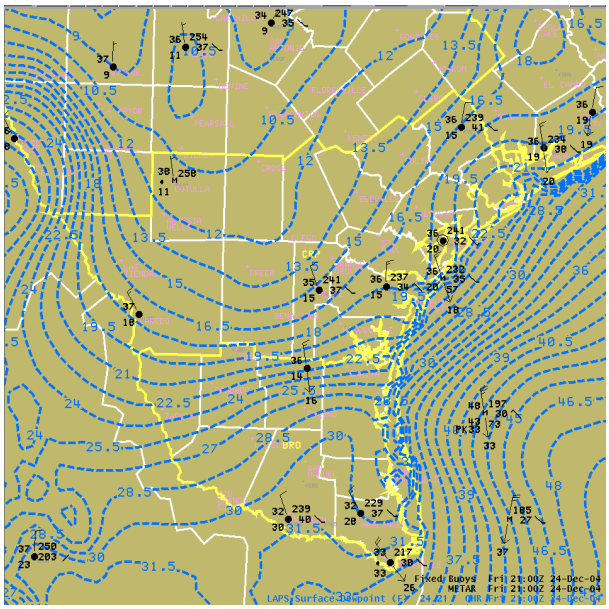

Figure 7. Surface metar and buoy data (black), and LAPS analysis of surface dew point temperatures (blue dashed lines). Temperatures in ˚F. Yellow lines denote CWA boundaries. Valid 2100 UTC 24 December.

By 0600 UTC, which was around the time of peak snow intensities, there was generally neutral to slightly negative (cold) temperature advection over all of south Texas between 850 and 500 hPa (not shown). Therefore, the combination of evaporative cooling due to precipitation falling into the drier air in the lowest 50 to 100 hPa, along with adiabatic cooling due to the intensifying ascent associated with the approaching upper trough and associated jet streak circulations, was likely enough to offset the weak mid level warm advection. This allowed temperatures to remain sufficiently cold enough for frozen precipitation to occur across all of south Texas. It was the presence of this deep cold air mass that was considered to be quite rare by many south Texas forecasters.

4. DIAGNOSIS OF THE HEAVY SNOW BAND

Beginning at 0000 UTC 25 December, the cross section taken perpendicular through the heavy snow band, revealed an axis of frontogenesis gently sloping from east to west in the layer between 850 and 700 hPa (Fig. 11, red line). The ageostrophic vertical circulation (not shown) produced by this lower to mid level axis of frontogenesis appeared to be the main mesoscale source of ascent within the banded region. In

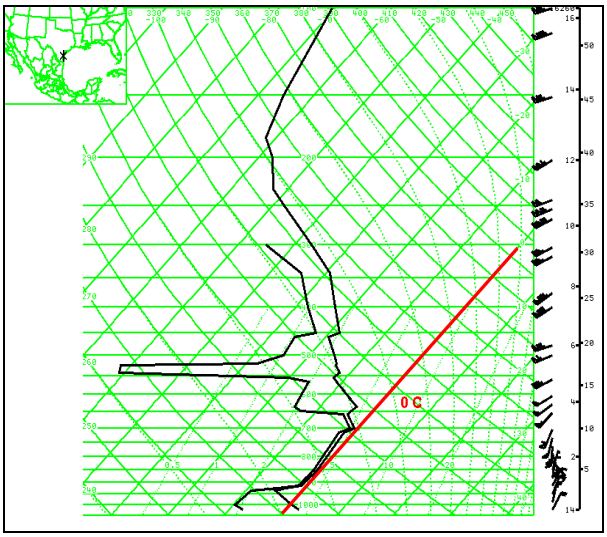

Figure. 8. Skew *T*-log p sounding from WFO CRP for 1200 UTC 24 December. The red line denotes the 0 ˚C isotherm.

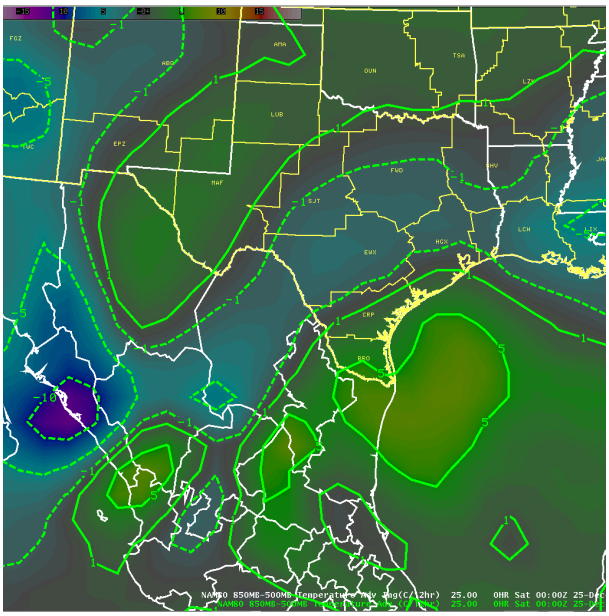

Figure 9. 850 to 500 hPa thermal advection (˚C 12 hr $^{-1}$), ending at 0000 UTC 25 December from the 80 km NAM-Eta. Yellow and green shaded regions denote warm advection, blue shaded regions cold advection.

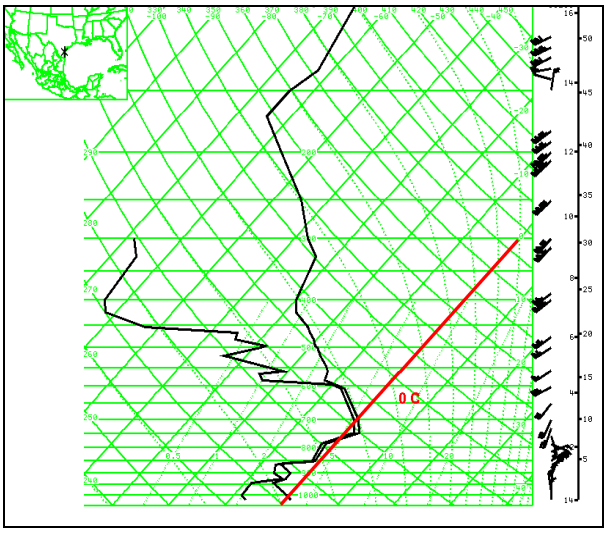

Figure 10. As Fig. 7, except for 0000 UTC 25 December.

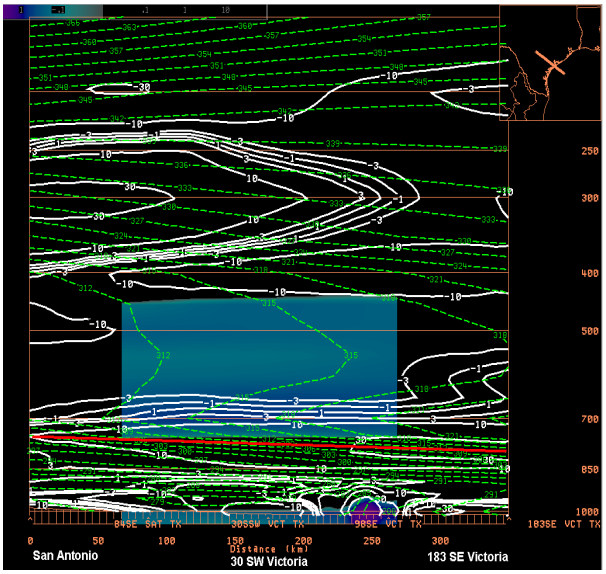

Figure 11. LAPS cross section at 0000 UTC 25 December perpendicular to the primary snow band (along red line Fig. 10) showing Petterssen frontogenesis (white contours, x 10 $^{-10}$ K m $^{-1}$ s $^{-1}$), saturated equivalent potential temperature (green dashed line, K), and saturated geostrophic potential vorticity (negative values shaded, units of PVU). The red line marks the axis of maximum frontogenesis of concern. White text labels along the x-axis denote three reference points along the cross section.

addition, this saturated, frontogenetic region was also embedded within an environment of deep synoptic scale ascent (Fig. 12) due to the approaching upper level trough and embedded jet streaks discussed in section 3. The region within the heavy snow band remained saturated (RH > 80%) through the event. Saturated conditions in the lower to mid levels were not only necessary for the production of pecipitation, but also for the existence of either conditional instability (CI) or conditional symmetric instability (CSI).

Just above the axis of frontogenesis, there was a large region of negative, saturated geostrophic equivalent potential vorticity (EPV*) of -0.5 to -1.0 PVU (Fig. 11), which signified the potential for enhanced, banded ascent above the axis of frontogenesis. The θ_{es} surfaces just above the frontogenesis axis were showing a decrease with height, indicating the presence of CI. Therefore, despite negative values of EPV*, the stability favored upright convection and the release of CI rather than CSI to enhance the heavy snow region. A preliminary study of this case by Becker et al. (2004) also supported this conclusion. This illustrated the drawback of looking only for the existence of negative EPV values to diagnose, or even forecast, the presence of CSI.

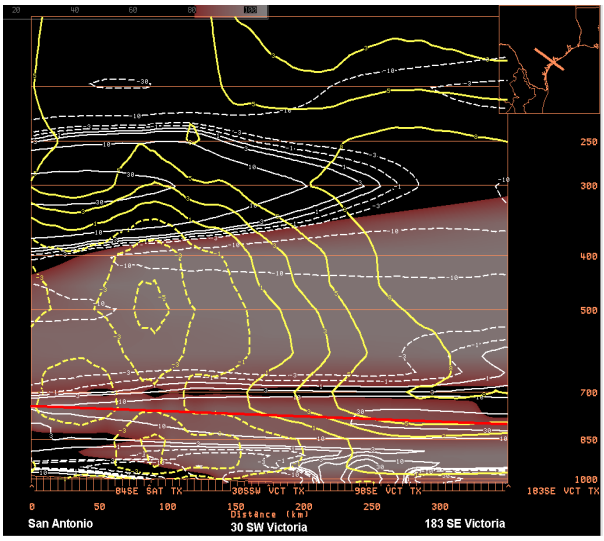

Figure 12. LAPS cross section at 0000 UTC 25 December along the same line as Fig. 10 depicting Petterssen Frontogenesis (white contours, x 10 $^{-10}$ K m $^{-1}$ s $^{-1}$, Omega (solid yellow lines are upward vertical motion, microbars s $^{-1}$), and RH ($\geq$ 80% shaded).

The origin of the CI region above the heavy snow band zone at 0000 UTC 25 December likely stemmed from the dry conveyor belt wrapping around the south and east side of the upper low, as seen in the water vapor imagery (Fig. 5a). This scenario is typically observed on the eastern side of a developing extra-tropical cyclone (Carlson 1980). The advection of drier air aloft over the moist/saturated lower to mid level layer helped to increase the slope of θ_e / θ_{es} surfaces above the mid level frontogenetic zone. The decreasing moisture during this time at mid levels above the heavy banded snow region could have potentially lead to better chances for CSI (Moore and Lambert 2003). However, the drying was strong enough to cause the θ_{es} surfaces to not only become more vertically sloped, but to decrease with height (i.e., CI). Reports of thunder did seem to fit well with the conclusion that CI was being release through upright convection. However, thunder alone may not necessarily preclude the existence of CSI and slantwise convection (Holle et al. 1996).

The other significant contributor to the negative values of EPV was the strong vertical wind shear. Winds from the 0000 UTC 25 December CRP sounding (Fig. 10) were generally from the southwest, increasing from around 15 m s^{-1} at 750 hPa, to more than 70 m s^{-1} at 300 hPa. Increasing winds with height were shown by Martin et al. (1992) and Moore and Lambert (1993) to be favorable for the production of negative EPV, and the potential for CSI.

By 0300 UTC 25 December, surface observations indicated that the precipitation had transitioned from light to heavy snow, and the KCRP 88D depicted a more stratiform nature to the precipitation (Figs. 6b, c). The cross section at this time continued to reveal a deep region of negative EPV* near and above the mid level frontogenetic zone (Fig. 13). In addition, the θ_{es} surfaces were still decreasing with height, which continued to indicate the potential for upright convection to be dominant. However, this layer of CI was higher and shallower compared to 0000 UTC, with flatter θ_{es} surfaces near the top of the frontal zone.

By 0600 UTC 25 December, the cross section showed that a region of negative EPV* near and above the mid level frontogenetic zone remained in place, but the magnitude and extent (horizontal and vertical) of the negative EPV region had decreased from 0300 UTC (Fig. 14). Also, the θ_{es} surfaces were much more horizontal above the frontal zone, and no longer decreasing with height. Given the evolution to flatter θ_{es} surfaces in the region above the frontogenesis zone at this time, the heavy snow was likely the result of enhanced slantwise ascent from the release of CSI on the warm side of the frontal zone. A cross section two hours earlier at 0400 UTC (not shown) revealed that the θ_{es} surfaces were no longer decreasing with height above the frontogenetic zone. Therefore, the banded heavy snow region appeared to transition from the release of CI through upright convection, to the release of CSI through enhanced slantwise upward motion around 0400 UTC.

As stated earlier, the heaviest snow fell between 0200 and 0800 UTC 25 December. Therefore, for approximately half of this six hour period, conditions were favorable for the release of CSI, and enhanced slantwise ascent in the heavy band region. The coverage and intensity of snowfall began to steadily decrease after 0800 UTC 25 December, as the large scale upper trough and upper level jet began to move east of the region (Fig. 4).

An additional factor that may have played a role in the increased snowfall rates within the heavy banded region was the potential for aggregation of snow crystals. Looking at the 0000 UTC 25 December CRP sounding (Fig. 10), the temperatures within the suspected snow production layer (750-600 hPa) were between 0˚C and -8˚C. This temperature range has been shown to be favorable for the aggregation of snow flakes, and the production of heavier snowfall rates (Baumgardt, 1999). Unfortunately, there were no reports indicating the size of the snow flakes within the heavy snow band region, which made it difficult to verify this theory.

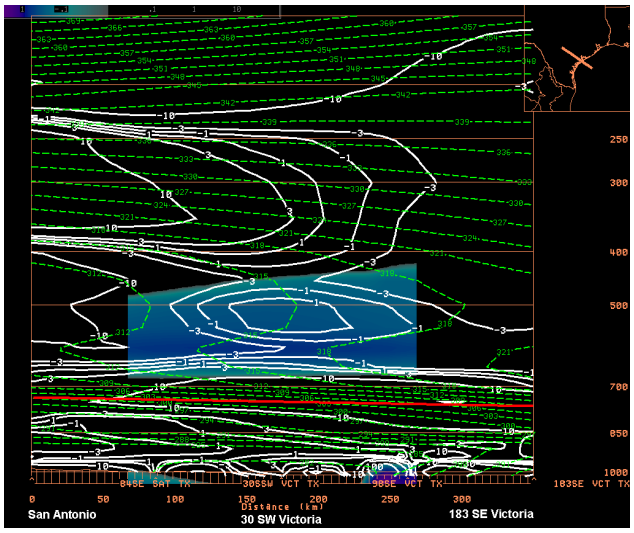

Figure 13. As in Fig. 11, except for 0300 UTC 25 December.

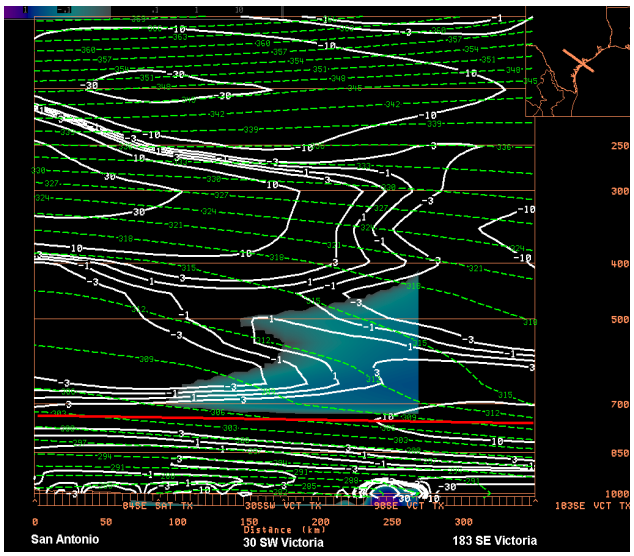

Figure 14. As in Fig. 11, except for 0600 UTC 25 December.

5. DISCUSSION AND CONCLUSIONS

For the first few hours of the event, the θ_{es} surfaces were decreasing with height just above the low to mid level frontogenesis axis, indicating the presence of CI, and therefore the likelihood that upright convection was dominant within the heavy snow band region. By 0300 UTC 25 December, the cross sections still showed the θ_{es} surfaces decreasing with height (i.e., "folding back"), but the depth of the decrease was shallower, and was no longer located just above the frontogenesis axis. By 0600 UTC, the θ_{es} surfaces were no longer folding back, and showed a more gradual/horizontal slope upward from east to west. This indicated more conditionally stable conditions, which have been observed to be more typical within regions of CSI. In addition, the bands were aligned parallel to the 1000-500 hPa thickness gradient (Fig. 3, bottom right), which has typically been observed within banded regions that result from the release of CSI. Therefore, between 0400 and 0600 UTC (about four hours into the event), there appeared to be a transition from the release of CI through upright convection, to the release of CSI and enhanced slantwise ascent within the heavy snow band.

This evolution toward a more convectively stable regime favorable for CSI seemed logical, given that the atmosphere has a natural tendency to become more stable in the presence of upward vertical motions. Emanuel (1983) proposed a different transition of the stability within the warm side of a frontal circulation, in which a two-dimensional circulation resulted in θ_e surfaces becoming over-turned (i.e., convectively unstable). This type of scenario could occur within the upper branch of frontal circulation along the warm side of a frontal zone. The top branch of this circulation could act to fold the θ_e surfaces with time, creating a more convectively unstable environment. However, for this case it appeared that the environment within the frontal zone and heavy snow band transitioned from that of weak conditional instability, to that of conditional symmetric instability.

Forecasting the timing, extent and intensity of such a heavy banded snow event continues to challenge operational forecasters and numerical weather prediction (NWP) models. Even if forecasters are well versed in the theories and procedures for forecasting heavy banded snow events, they can be mislead by NWP models, which have generally lacked the proper resolution to accurately predict the timing and placement of the heavy precipitation band. For this event, all of the available operational NWP models greatly under-forecast the location of the maximum precipitation, placing it well offshore into the Gulf of Mexico. Thus, in addition to being a rare event, the available NWP guidance was very poor.

Over the past few years, the horizontal resolutions of mesoscale models have dramatically increased. For example, the operational Meso-Eta/NAM (North American Model) at the time of this event had a horizontal grid spacing of 12 km. However, numerical simulations by Persson and Warner (1993) showed that in order for a model to explicitly resolve the circulations of intense, extremely narrow (less than 30-40 km) bands associated with the release of CSI, model horizontal grid resolutions of 5 to10 km would be required.

Schumacher (2003) devised a methodology for forecasters to predict the potential for meoscale bands in an operational setting. This methodology begins with examining the potential for upper level forcing by either looking at Q-vector convergence between 300 to 400 hPa, or tropopause pressure advection. Next, the forecaster diagnoses 50 hPa layer averages of frontogenesis, or single layers between 900 and 600 hPa, to determine where the interaction between the upper level forcing and the frontal boundary will be maximized. Finally, once the level or layer is determined, EPV is examined above the frontal surface to determine the potential for banded precipitation. For more specific details pertaining to this method, refer to sections 5 and 6 of the National Weather Service's Winter AWOC training, produced by the Warning Decision Training Branch (WDTB).

More recently, Novak et al. (2006) demonstrated the success of NWS forecasters to accurately forecast the timing and approximate location of heavy snow band(s) up to 12 hours in advance across the northeast U.S., using models such as the Workstation Eta/NAM and the MM5 (PSU/NCAR Mesoscale Model). A strategy for operational forecasters was developed, based on the basic theory that mesoscale banded precipitation is typically associated with frontogenesis, weak symmetric stability, and sufficient moisture. This forecast strategy was similar to the diagnostic techniques used in this study. Within 24 hours of the event, the scheme focuses on plan view forecasts of mid level frontogenesis. Assuming saturation and weak symmetric stability (i.e., small or negative EPV), the axis of mid level frontogeneis has been shown to correlate well with the heavy band location (Novak et al. 2006). However, as was seen with cross sections in this and other studies, frontogenesis usually slopes with height through the heavy banded region. Thus, it is suggested that forecasters use cross sections through the area of interest to help direct which level (or layer) of frontogenesis to display on horizontal maps. Once the general region for the potential band is determined, cross sections perpendicular to the band could be utilized to determine the distribution of EPV, stability and the potential for CSI at least 12 to 24 hours prior to the event.

In conclusion, this study not only documented that heavy banded snow can occur at very low latitudes (i.e., south of 30˚N), but also demonstrated that techniques developed to diagnose banded events at higher latitudes could be successfully applied. Although heavy banded snowfall events are rare across south Texas, presumably due to the lack of deep, sufficiently cold air, it is theorized that banded heavy rainfall events may be more frequent. Additional case studies are needed to determine if the techniques, such as those outlined in this study could be used for heavy banded rainfall events.

ACKNOWLEDGEMENTS

The author appreciates David "Rusty" Billingsley's efforts with reviewing this study at the Southern Region's Science and Training Branch of the National Weather Service. In addition, the author thanks Phil Schumacher (Science and Operations Officer WFO Sioux Falls, SD), and Michael Evans (Science and Operations Officer WFO Binghamton, NY), for their detailed reviews. Also, Tony Merriman's (Intern WFO CRP) efforts with producing the high quality snowfall analysis map and with post editing, was greatly appreciated. Much of this paper would not have been possible without the countless hours of editing help from Greg Wilk (Lead Forecaster WFO CRP). Finally, the author is thankful for the comments from two anonymous reviewers.

REFERENCES

Albers, S., J. McGinley, D. Birkenheuer, and J. Smart, 1996: The Local Analysis and Prediction System (LAPS): Analysis of clouds, precipitation, and temperature. *Wea and Forecast*, **11**, 273-287.

Baumgardt, D., 1999: Wintertime cloud microphysic review. NWS La Crosse, WI web page, http://www.crh.noaa.gov/arx/micro/micrope.php

Becker, A., B. P. Pettegrew, C. J. Melick, L. L. Smith, C. Schultz, P. Buckley, A. Lupo, and P. Market: A Case Study of the Gulf Coast Thundersnow Event of Christmas 2004. A*bstract* 30th annual National Weather Association's meeting15-20 october 2005, Saint Louis, MI.

Carlson, T. N., 1980: Airflow through midlatitude cyclones and the comma cloud pattern. *Mon. Wea. Rev.*, **108**, 1498-1509.

Emanuel, K. A., 1983: The lagrangian parcel dynamics of moist symmetric instability. *J. Atmos. Sci.*, **40**, 2368-2376.

Griffths, J. F., G. Ainsworth, 1981: One hundred years of Texas weather 1880-1979, Mongraph Series No. 1, Office of the State Climatologist Department of Meteorology, College of Geosciences, Texas A & M University.

Holle, R. L., and A. I. Watson, 1996: Lightning during two central U.S. winter precipitation events. *Wea. Forecasting*, **11**, 599-614.

Jurewicz, M. L., and M. S. Evans, 2004: A comparison to two banded, heavy snowstorms with very different synoptic settings. *Wea. Forecasting*, **19**, 1011-1028.

Martin, J. E., J. D. Locatelli, and P. V. Hobbs, 1992: Organization and structure of clouds and precipitation on the mid-Atlantic Coast of the United States. Part V: The role of an upper-lvel front in the generation of a rainband. *J. Amos. Sci.*, **49**, 1293-1303.

Moore, J. T., and T. E. Lambert, 1993: The use of equivalent potential vorticity to diagnose regions of conditional symmetric instability. *Wea. Forecasting*, **8**, 301-308.

National Climatic Data Center (NCDC), December 2004: Storm Data and Unusual Weather Phenomena, **Vol 46**, Number 12 (www.ncdc.noaa.gov)

Nicosia, D. J., and R. H. Grumm, 1999: Mesoscale band formation in three major Northeastern United States snowstorms. *Wea. Forecasting*, **14**, 346-368.

Novak, D. R., J. S. Waldstreicher, L. F. Bosart, and D. Keyser, 2006: A forecast strategy for anticipating cold season mesoscale band formation within Eastern U.S. cyclones. *Wea. Forecasting*, **21**, 3-23.

Novak, D., and G. Wiley, 2002: Mesoscale Snowband Cross Section, AWIPS Technical Note 5.0-42, 9 pp.

Persson, P. O. G., and T. T. Warner, 1993: Nonlinear hydrostatic conditional symmetric instability: Implications for numerical weather prediction. *Mon. Wea. Rev.,***121**, 1821-1833.

Schultz, D. M., P. N. Schumacher, 1999: The use and misuse of conditional symmetric instability. *Mon. Wea. Rev*., **127**, 2709-2732.

Schumacher, P. N., 2003: An example of forecasting mesoscale bands in an operational environment. *Preprints, 10th Conf. on Mesoscale Processes, Portland, OR, Amer. Meteor. Soc.*, CD-ROM, P8.1.

Wilk, G. E., R. F. Morales, J. Runyen, R. Burton 2007: The Historic Christmas 2004 South Texas Snow Event: Model Performance, Forecaster Response, and Public Perception. *NOAA/NWS Southern Region Technical Memorandum*.